2-(1H-pyrazol-3-yl)pyrazine: a polytopic N-donor ligand used to construct Cu-[2+2] molecular grid: synthesis, structure, and magnetic properties

Xue-Feng Feng [a] , Chuo Yang [a] , Zhen-Wei Liao [a] , Yu-Mei Song [a] , Hai-Xiao Huang [a] , Gong-Ming Sun [a] , Ming-Biao Luo [a] , Shu-Juan Liu [a] & Feng Luo [a]

[a] College of Biology, Chemistry and Material Science, East China Institute of Technology , Fuzhou , Jiangxi , China
Published online: 06 Dec 2011.

PLEASE SCROLL DOWN FOR ARTICLE

2-(1H-pyrazol-3-yl)pyrazine: a polytopic N-donor ligand used to construct Cu-[2 + 2] molecular grid: synthesis, structure, and magnetic properties

XUE-FENG FENG, CHUO YANG, ZHEN-WEI LIAO, YU-MEI SONG,
HAI-XIAO HUANG, GONG-MING SUN, MING-BIAO LUO, SHU-JUAN LIU
and FENG LUO*

College of Biology, Chemistry and Material Science, East China Institute of Technology,
Fuzhou, Jiangxi, China

Herein, we present a new polytopic N-donor, which is used to construct a metal–organic compound. The resulting metal–organic compound, $Cu_4(L)_6(NO_3)_2$ (HL=(1H-pyrazol-3-yl)pyrazine) (**1**), is synthesized by the hydrothermal reaction of $Cu(NO_3)_2$ and HL (ratio: 1:1). Single-crystal X-ray diffraction shows that **1** comprises a Cu-[2+2] molecular grid. Magnetic studies reveal antiferromagnetic interactions, interpreted by a simplified dinuclear mode.

Keywords: Hydrothermal synthesis; Polytopic ligand; [2+2] Molecular grid; Magnetic property

1. Introduction

Efforts have been devoted to design the molecular grid-type complexes that are an interesting class of compounds in the area of nanoscale materials for their potential to exhibit architecture-dependent behavior (e.g. molecular magnetism, host-guest properties, catalysis) [1–3]. A successful approach to design such materials is to achieve control over the self-assembly involving a ligand system [4–6]. The choice of ligand lies in two main factors, namely, rigidity (to minimize variability) and the use of polytopic coordination sites (to ensure multiple metal centers are coordinated) (e.g. pyridazine, pyrimidine, phenoxide) [7–14]. N^3-(2-pyridoyl)-2-pyridinecarboxamidrazone and analogs are often employed to construct homometallic or heterometallic [2+2] molecular grids [1–3].

As shown in scheme 1, a new polytopic N-donor, 2-(1H-pyrazol-3-yl)pyrazine (HL), containing both heterocyclic pyrazole and pyrazine has the potential to provide four N-donor coordination sites. According to the above criteria required for ligands, the rigidity is present, whilst a chelate site plus additional possible coordination can expand the ligand to connect to more than one metal. The extending site can produce

---

*Corresponding author. Email: ecitluofeng@163.com

Extending site

Coordination site

Chelate site

2-(1H-pyrazol-3-yl)pyrazine
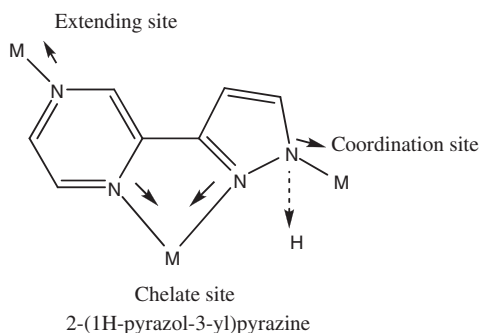
Scheme 1. The coordination potential of L; M is metal ion.

low-dimensional to high-dimensional architectures. A query of the CCDC (CSD, February 2011 release) reveals no metal–organic compounds built using this ligand. We herein report the hydrothermal self-assembly of HL and Cu(II) resulting in a Cu-[2+2] molecular grid-type compound. Magnetic properties of the system are also discussed.

2. Experimental

2.1. *Materials and methods*

Commercially available reagents were used as-received. Magnetic measurements were carried out with a Quantum Design (SQUID) magnetometer MPMS-XL-5.

2.2. *Synthesis of 1*

A solution (6 mL water) of $Cu(NO_3)_2$ (0.1 mmol) and HL (0.1 mmol) was sealed in a Teflon reactor, heated at 160°C for 2 days, and then cooled to room temperature at $3°C\,h^{-1}$. Blue crystals were obtained in 82% yield based on HL. Elemental Anal Calcd: C 40.38, N 29.16, H 2.42; exp. C 40.33, N 29.17, H 2.43.

2.3. *Crystallographic data for 1*

A single crystal of **1** was mounted in air onto thin glass fibers. Unit cell parameters were determined by a least-squares fit of 2θ values and intensity data were measured on a Bruker CCD area detector diffractometer with Mo-Kα radiation ($\lambda = 0.71073\,\text{Å}$) at room temperature. The intensities were corrected for Lorentz and polarization effects as well as for empirical absorption based on multi-scan technique. The structure was solved by direct methods and refined by full-matrix least-squares fitting on F^2 by SHELX-97. All non-hydrogen atoms were refined with anisotropic thermal parameters. Crystallographic data for **1** is summarized in table 1. Selected bond lengths and angles are listed in table 2.

Table 1. Crystallographic data and structure refinement details for **1**.

	1
Empirical formula	$C_{21}H_{15}Cu_2N_{13}O_3$
Formula weight	624.54
Temperature (K)	296(2)
Crystal system	Monoclinic
Space group	$P2_1/c$
Unit cell dimensions (Å, °)	
a	10.4150(3)
b	21.4150(7)
c	10.8862(4)
β	95.390(3)
Volume (Å^3), Z	2417.29(14), 4
$F(000)$	1256
Reflections collected	18,568
Independent reflection	4258 [R(int) $= 0.0742$]
Calculated density (g cm^{-3})	1.716
S	1.045
R indices (all data)	$R_1 = 0.0890$, $wR_2 = 0.1459$

Table 2. Selected bond lengths (Å) and angles (°) for **1**.

Cu(1)–N(2)	1.964(5)	N(11)–Cu(1)–N(12)	79.84(19)
Cu(1)–N(6)	1.973(4)	N(2)–Cu(1)–N(3)	74.09(19)
Cu(1)–N(11)	1.976(5)	N(6)–Cu(1)–N(3)	95.56(18)
Cu(1)–N(12)	2.065(5)	N(11)–Cu(1)–N(3)	114.45(19)
Cu(1)–N(3)	2.451(5)	N(12)–Cu(1)–N(3)	89.02(17)
Cu(2)–N(10)	1.952(5)	N(10)–Cu(2)–N(7)	96.06(19)
Cu(2)–N(7)	1.990(5)	N(10)–Cu(2)–N(8)	173.4(2)
Cu(2)–N(8)	2.015(5)	N(7)–Cu(2)–N(8)	81.45(19)
Cu(2)–N(5)#1	2.062(5)	N(10)–Cu(2)–N(5)#1	95.0(2)
Cu(2)–O(1)	2.228(14)	N(7)–Cu(2)–N(5)#1	126.2(2)
N(2)–Cu(1)–N(6)	89.94(19)	N(8)–Cu(2)–N(5)#1	91.3(2)
N(2)–Cu(1)–N(11)	167.74(19)	N(10)–Cu(2)–O(1)	90.7(3)
N(6)–Cu(1)–N(11)	97.66(19)	N(7)–Cu(2)–O(1)	105.7(4)
N(2)–Cu(1)–N(12)	91.88(19)	N(8)–Cu(2)–O(1)	84.1(3)
N(6)–Cu(1)–N(12)	175.4(2)	N(5)#1–Cu(2)–O(1)	126.6(4)

Symmetry code: #1 $= -x+1, -y+1, -z+2$.

3. Results and discussion

3.1. *Crystal structure of 1*

Compound **1** was synthesized by hydrothermal self-assembly of Cu(NO$_3$)$_2$ and L at 160°C. The single crystal X-ray diffraction study reveals that **1** crystallizes in the monoclinic space group $P2_1/c$. The asymmetric unit contains two crystallographically-independent Cu(II) ions, three deprotonated L, and one structure-disordered NO$_3^-$. Both Cu1 and Cu2 sites are five-coordinate, yet exhibit different coordination geometries. Cu1 has a highly distorted CuN$_5$ square pyramidal geometry that is completed by five nitrogen atoms from three different ligands wherein N2, N6, N11, N12 form the basal quadrangular plane and N3 is located on the axis with a large offset (N3–Cu1–N2 angle of *ca* 74° is smaller than the expected value of 90° for a regular
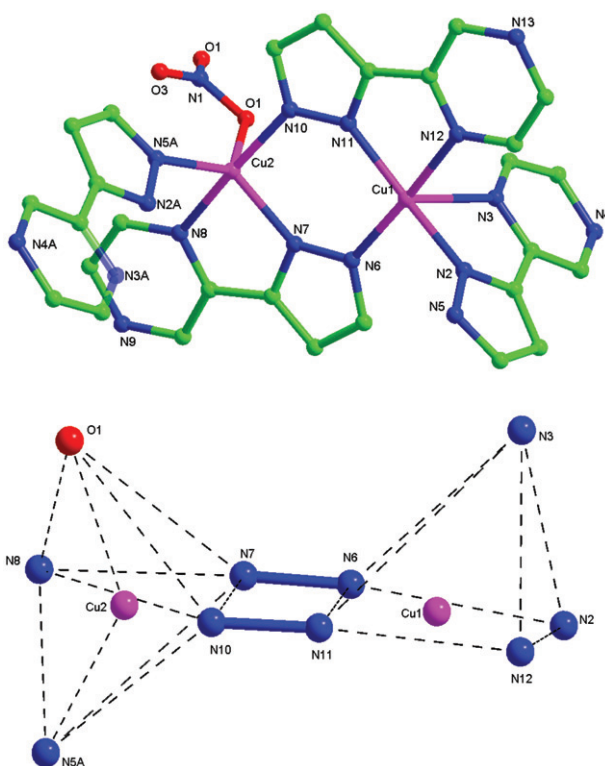
Figure 1. The asymmetric unit of **1** and coordination geometry of copper ions **1**. Hydrogen atoms are omitted for clarity.

square pyramid). The Cu1–N3 bond length of 2.451(5) Å is longer than other Cu1–N bond lengths, Cu1–N2: 1.964(5) Å, Cu1–N6: 1.973(4) Å, Cu1–N11: 1.976(5) Å, Cu1–N12: 2.065(5) Å, indicating an axis-elongated square pyramidal geometry for Cu1. By contrast, the Cu2 site affords a distorted CuN_4O trigonal bipyramidal geometry, completed by N7, N8, and N10 from two L that create the equatorial plane, and O1, N5A $(1 - x, 1 - y, 2 - z)$ from one L and one NO_3^- are situated on the axis but with large offset (O1–Cu2–N5A angle of *ca* 126.6° is smaller than the expected value of 180° for the regular trigonal bipyramid). The Cu–O1/N5A bond lengths of 2.23(14) Å, 2.062(5) Å are slightly longer than Cu–N7/N8/N10 bond lengths of 1.990(5) Å, 2.015(5) Å, 1.952(5) Å, indicating an axis-elongated phenomenon (figure 1).

As shown in figures 1 and 2, Cu1 and Cu2 are bridged by double N_2 bridges of L to create the Cu_2 dimer. Two symmetry-related dimer fragments are combined by double N_2 bridges of L that result in an overall Cu-[2+2] molecular grid wherein the Cu1-to-Cu2 and Cu1-to-Cu2A distances are 3.964(1) Å and 3.5873(1) Å. The ligands have tridentate coordination with two N-donors chelating, one being an uncoordinated nitrogen outside of the Cu-[2+2] molecular grid. The "cavity" of the grid is quite small and not expected to act as a host.

A comparison with well-characterized Cu-[2+2] molecular grids shows several differences [1–3]. Compound **1** involves six L, rather than four ligands observed in the literature, implying more magnetic coupling pathways. Among the reported cases, the
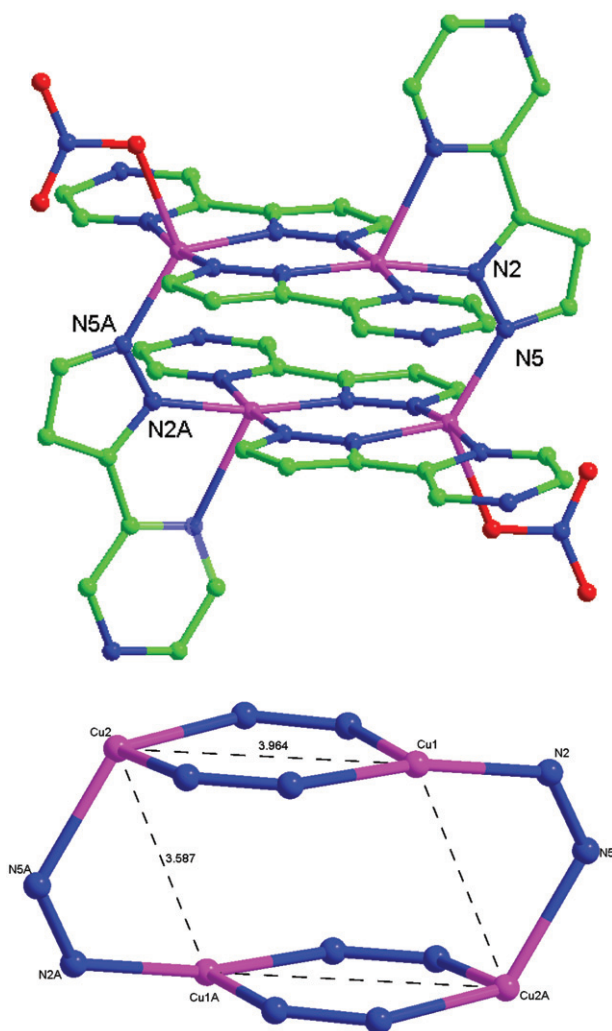
Figure 2.　View of the Cu-[2+2] molecular grid in **1**.

single O-bridge prevails, and only limited examples contain both single O-bridge and single N_2 bridges. By contrast, the present one presents the first Cu-[2+2] molecular grid connected by only N_2 bridges.

3.2. *IR and magnetic studies*

IR peaks at 3174, 1356, 1051, 926, and 613 cm^{-1} for **1** are ascribed to the pyrazol group, whereas peaks at 1615, 1505, 1432, 1146, and 797 cm^{-1} are typical of the pyrazine group. The peak at 1383 cm^{-1} is derived from NO_3^-.

The temperature-dependent magnetic susceptibility data of **1** was measured for crystal samples at an applied magnetic field of 500 Oe from 2.7 to 300 K. The $\chi_M T$ value
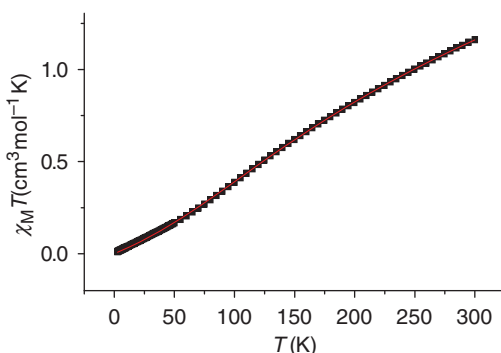
Figure 3. The exp./dot and simulated/line $\chi_M T$ *vs. T* plots.

at room temperature is $1.16\,\mathrm{cm^3\,mol^{-1}\,K}$, smaller than the expected value of $1.5\,\mathrm{cm^3\,mol^{-1}\,K}$ for four isolated Cu(II) centers ($g = 2.0$, $S = 1/2$), owing to strong antiferromagnetic interactions. Upon cooling, the $\chi_M T$ values decrease until $2.7\,\mathrm{K}$ of $0.01\,\mathrm{cm^3\,mol^{-1}\,K}$, indicating the strong antiferromagnetic behavior (figure 3).

To evaluate the order of magnitude of the antiferromagnetic coupling mediated by N_2 bridges of L, a well-known isotropic tetramer mode by means of $H = -2J_1(S_{Cu2} \cdot S_{Cu1} + S_{Cu2A} \cdot S_{Cu1A}) - 2J_2(S_{Cu1A} \cdot S_{Cu2} + S_{Cu1} \cdot S_{Cu2A})$ is used to analyze the temperature-dependent magnetic susceptibility data. However, the attempts only resulted in ill-defined interaction constants, with too little data to define the parameters (e.g. high temperatures). We considered a simplified dimer isotropic mode upon $H = -2J_1 S_{Cu2} \cdot S_{Cu1}$ with the considerations of intra- and inter-tetramer interactions of θ.

$$\chi_M = (1 - \rho)\frac{2N_A\beta^2 g^2}{k_B(T - \theta)}[3 + \exp(-J/K_B T)]^{-1} + 2\rho N_A \beta^2 / k_B / T + \mathrm{TIP}$$

The best fit of $\chi_M T$ *versus T* plots at 300–2.7 K gives $J = -318.2\,\mathrm{cm^{-1}}$, $g = 2.0$, $\mathrm{TIP} = 630 \times 10^{-6}\,\mathrm{cm^3\,mol}$, $\theta = -83.3\,\mathrm{K}$, $\rho = 0.08$, where J is the intra-dimer coupling constant between Cu2–Cu1 and Cu2A–Cu1A, θ is the intra- and inter-tetramer interactions, g the Zeeman factor, TIP the temperature-independent paramagnetism and ρ paramagnetic impurities [15]. The result suggests strong antiferromagnetic interactions between Cu2–Cu1 and Cu2A–Cu1A and relatively weaker antiferromagnetic interactions between Cu1–Cu2A and Cu1A–Cu2. By comparing with reported Cu-[2+2] complexes, the strong antiferromagnetic interactions between Cu2–Cu1 and Cu2A–Cu1A are comparable, whereas the large antiferromagnetic interactions between Cu1–Cu2A and Cu1A–Cu2 are not typical, as the coupling pathway does not involve $d_{x^2-y^2}$-like single-output, multiple-output orbital and is usually invalid [16–19].

No obvious magnetic coupling between Cu1–Cu2A and Cu1A–Cu2 is observed in the literature in similar Cu-[2+2] molecular grids, as in this coupling pathway the magnetic coupling is invalid owing to a single electron occupying the local plane of $d_{x^2-y^2}$ orbital rather than the axis d_{z^2} orbital [15]. However, based on the simulated results, it is obvious that distinct magnetic behavior with obvious magnetic coupling between Cu1–Cu2A and Cu1A–Cu2 is observed in **1**. To further understand the magnetic properties of **1**, a detailed magneto–structure relationship is discussed below.

For Cu1 with the square pyramidal geometry and Cu2 with trigonal bipyramid geometry, the expected hybridization of the metal atom is dsp^3; however, the nonbonding and antibonding orbitals are very different. The antibonding orbital of Cu1 is $d_{x^2-y^2}$, whereas that of Cu2 site is d_{z^2}. The analysis means that only a single electron occupies the $d_{x^2-y^2}$ orbital for Cu1 and d_{z^2} orbital for Cu2. Between Cu1–Cu2 and Cu1A–Cu2A, the magnetic interactions is between the magnetic orbital located in plane for Cu1, Cu1A and the magnetic orbital located on the axis for Cu2, Cu2A, where no magnetic orbital orthogonality can be built. Similar situation is observed within Cu1–Cu2A and Cu1A–Cu2. Furthermore, based on orthogonalization and the nature of the magnetic orbital approach, the $d_{x^2-y^2}$ and d_{z^2} orbitals are denoted as *a*1 and *a*1′. Then the magnetic interaction is determined by $J_{a1a1'}$, which involves no orthogonal orbitals. Thereby, there is no possibility of accidental orthogonality and $J_{a1a1'}$ is expected to be significantly anti-ferromagnetic [15]. The result is consistent with the experimental and simulated results of $\chi_M T$ *versus* T plot.

4. Conclusions

In this work, a new polytopic N-donor ligand has been employed to form a metal–organic compound. The Cu-[2+2] molecular grid has been generated through the hydrothermal method. The present Cu-[2+2] molecular grids contain six ligands and magnetic coupling mediated by pure N_2 bridges. Unusual magnetic behavior is also notable and interpreted by hybridization theory, orthogonalization, and magnetic orbital approach. This work shows the new polytopic N-donor ligand to be effective in constructing multi-nuclear metal–organic compounds.

Acknowledgments

References

[1] M. Ruben, J. Rojo, F.J. Romero-Salguero, L.H. Uppadine, J.-M. Lehn. *Angew. Chem. Int. Ed.*, **3644**, 43 (2004).
[2] L.N. Dawe, K.V. Shuvaev, L.K. Thompson. *Chem. Soc. Rev.*, **2334**, 38 (2009).
[3] O. Waldmann. *Coord. Chem. Rev.*, **2550**, 249 (2005).
[4] L.K. Thompson, C.J. Matthews, L. Zhao, Z.Q. Xu, D.O. Miller, C. Wilson, M.A. Leech, J.A.K. Howard, S.L. Heath, A. Gavin Whittaker, R.E.P. Winpenny. *J. Solid State Chem.*, **308**, 159 (2001).
[5] C.J. Matthews, K. Avery, Z. Xu, L.K. Thompson, L. Zhao, D.O. Miller, K. Biradha, K. Poirier, M.J. Zaworotko, C. Wilson, A.E. Goeta, J.A.K. Howard. *Inorg. Chem.*, **5266**, 38 (1999).

 [6] L.N. Dawe, T.S.M. Abedin, T.L. Kelly, L.K. Thompson, D.O. Miller, L. Zhao, C. Wilson, M.A. Leech, J.A.K. Howard. *J. Mater. Chem.*, **2645**, 16 (2006).
 [7] L.N. Dawe, K.V. Shuvaev, L.K. Thompson. *Inorg. Chem.*, **3323**, 48 (2009).
 [8] L.N. Dawe, L.K. Thompson. *Angew. Chem., Int. Ed.*, **7440**, 46 (2007).
 [9] M. Barboiu, G. Vaughan, R. Graff, J.-M. Lehn. *J. Am. Chem. Soc.*, **10257**, 125 (2003).
[10] K.V. Shuvaev, S.S. Tandon, L.N. Dawe, L.K. Thompson. *Chem. Commun.*, **4755**, 46 (2010).
[11] G.N. Newton, T. Onuki, T. Shiga, Ma. Noguchi, T. Matsumoto, J.S. Mathieson, M. Nihei, M. Nakano, L. Cronin, H. Oshio. *Angew. Chem., Int. Ed.*, **4844**, 50 (2011).
[12] K.V. Shuvaev, T.S.M. Abedin, C.A. Mcclary, L.N. Dawe, J.L. Collins, L.K. Thompson. *Dalton Trans.*, 2926 (2009).
[13] C.J. Matthews, S.T. Onions, G. Morata, L.J. Davis, S.L. Heath, D.J. Price. *Angew. Chem., Int. Ed.*, **3166**, 42 (2003).
[14] L.K. Thompson, C.J. Matthews, L. Zhao, C. Wilson, M.A. Leech, J.A.K. Howard. *Dalton Trans.*, 2258 (2001).
[15] O. Kahn. *Molecular Magnetism*, VCH Publishers Inc., New York (1993).
[16] Z. Xu, L.K. Thompson, D.O. Miller. *Inorg. Chem.*, **3985**, 36 (1997).
[17] L.K. Thompson, Z. Xu, A.E. Goeta, J.A.K. Howard, H.J. Clase, D.O. Miller. *Inorg. Chem.*, **3217**, 37 (1998).
[18] Z. Xu, L.K. Thompson, D.O. Miller, H.J. Clase, J.A.K. Howard, A.E. Goeta. *Inorg. Chem.*, **3620**, 37 (1998).
[19] C.J. Matthews, K. Avery, Z.Q. Xu, L.K. Thompson, L. Zhao, D.O. Miller, K. Biradha, K. Poirier, M.J. Zaworotko, C. Wilson, A.E. Goeta, J.A.K. Howard. *Inorg. Chem.*, **5266**, 38 (1999).